

# IMPLEMENTATION OF COALESCENCE CRITERIA INTO THE GTN MODEL APPLICATION TO WORK-HARDENING DUCTILE MATERIALS

J. Chambert<sup>1,2</sup>, Ph. Bressollette<sup>1</sup> and A. Vergne<sup>1</sup>

<sup>1</sup> Laboratoire d'Etudes et de Recherches en Mécanique des Structures (LERMES),  
Université Blaise Pascal – Clermont-Ferrand II, 63177 Aubière, France

<sup>2</sup> Laboratoire de Recherches et Applications en Mécanique Avancée (LaRAMA),  
IFMA, Campus de Clermont-Ferrand / Les Cézeaux, 63175 Aubière, France

## ABSTRACT

Until now, there is no widely accepted procedure to identify the damage parameters of the Gurson-Tvergaard-Needleman (GTN) model. The practical application of this model is limited by the determination of its numerous parameters. Particularly the value of the critical porosity  $f_c$  is still an open question because it is difficult to obtain it experimentally or numerically. Another way to determine the  $f_c$  parameter is by including a void coalescence criterion based on physical considerations, in the GTN model. In this study, two criteria of void coalescence have been incorporated into the GTN model. These new models, called GTNT and GTNP, have been implemented in the FE code CASTEM 2000. The main purpose of this study is to investigate the ability of such local approach models to describe the ductile fracture of metals. These models were applied to simulate tensile tests on axisymmetric round specimens made of ferritic steel 16MND5 and austenitic steel 316L. Within these new models, the number of unknown parameters is reduced to one 'free' parameter, which is determined by comparing the numerical and the experimental results. At first glance, the GTNP model seems to provide more realistic  $f_c$ -values than the GTNT model.

## INTRODUCTION

Since classical fracture mechanics have not accurately predicted the geometric and loading effects, local approaches have been increasingly used to simulate ductile fracture. Gurson [1] has proposed a micro-mechanical model for porous ductile solid with a randomly distributed void volume fraction  $f$ , defined as a damage parameter. Tvergaard and Needleman [2] have modified the Gurson model in order to simulate the void coalescence process. Unfortunately, the GTN model is defined by many parameters. In this study, two new approaches based on the GTN model are proposed for fitting the damage parameters. These models have been tested on two types of steel (16MND5 and 316L) used in nuclear power plants.

## CONSTITUTIVE EQUATIONS

In this study, the overall ductile porous material is idealized by a periodic array of axisymmetric unit cells (see Figure 1a). Each axisymmetric cylindrical cell of current  $2H$ -height and  $L$ -radius contains a spherical microvoid of current  $R$ -radius, surrounded with von Mises matrix materials. Subsequently, the microscopic quantities concern the local state in the unit cell; they are represented by small letters ( $\sigma_{ij}$ ,  $\varepsilon_{ij}$ ). Capital letters ( $\Sigma_{ij}$ ,  $E_{ij}$ ) are used for the 'mesoscopic' conditions applied to the cell. Mesoscopic quantities are defined by averaging the

microscopic variables over the cell volume.

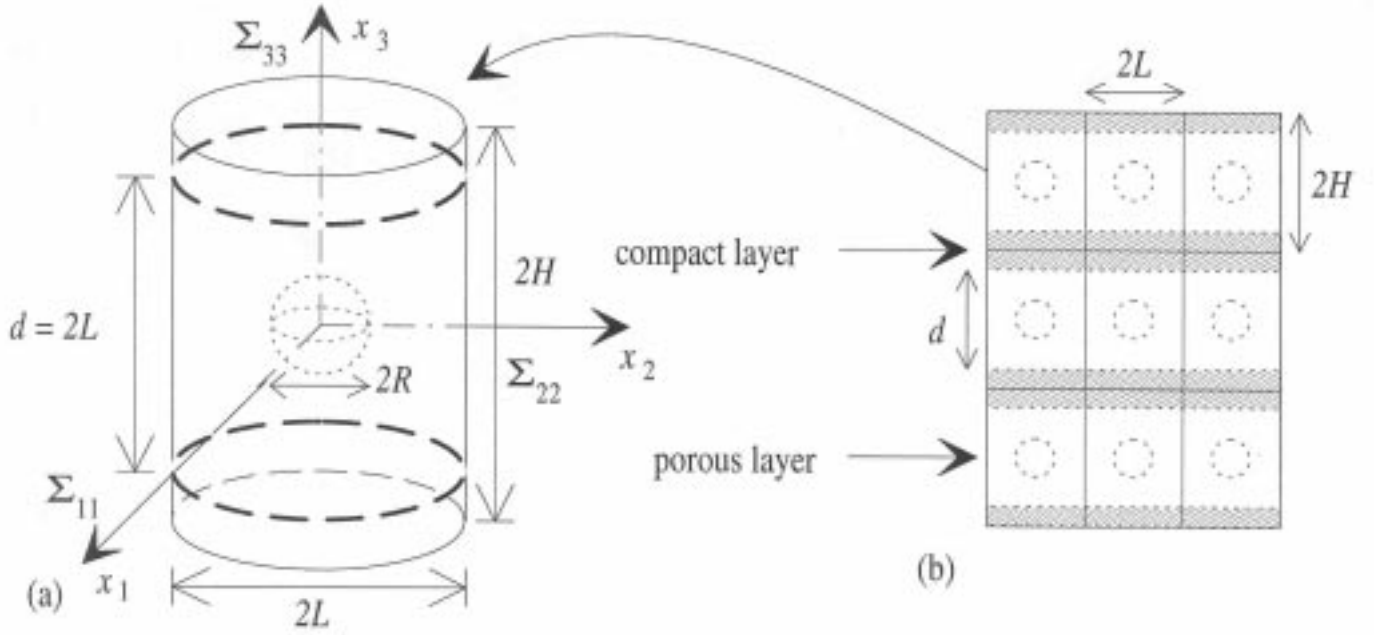


**Figure 1:** (a) Axisymmetric unit cell – (b) Porous/compact layers

### The GTN Model

The Gurson constitutive model for porous ductile materials as modified by Tvergaard and Needleman [2] is based on the yield condition:

$$\Phi(\Sigma_{ij}, \bar{\sigma}, f) = \frac{\Sigma_{eq}^2}{\bar{\sigma}^2} + 2q_1 f^* \cosh\left(\frac{3}{2} q_2 \frac{\Sigma_m}{\bar{\sigma}}\right) - 1 - (q_1 f^*)^2 = 0 \quad (1)$$

in which  $q_1$  and  $q_2$  are ‘constitutive’ parameters introduced by Tvergaard (in the following, we use the classical value  $q_2 = 1$ ),  $\Sigma_{ij}$  is the mesoscopic Cauchy stress tensor,  $\Sigma_{eq}$  denotes the equivalent stress, defined by  $\Sigma_{eq}^2 = 3 \Sigma'_{ij} \Sigma'_{ij} / 2$  with  $\Sigma'_{ij}$  being the stress deviator,  $\Sigma_m$  is the hydrostatic stress, given by  $\Sigma_m = \Sigma_{kk} / 3$ ,  $\bar{\sigma}$  is the flow stress of the matrix material. The function  $f^*$ , which depends on the void volume fraction  $f$ , was introduced by Tvergaard and Needleman [2] in order to account for void coalescence:

$$f^*(f) = \begin{cases} f & \text{si } f \leq f_c \\ f_c + \frac{f_U - f_c}{f_F - f_c} (f - f_c) & \text{si } f > f_c \end{cases} \quad (2)$$

Here,  $f_c$  is the critical value of porosity at which void coalescence begins. Coalescence is complete once  $f$  reaches the final void volume fraction  $f_F$ . The porosity rate comes partly from the growth of existing voids and partly from the nucleation of new voids:

$$\dot{f} = (1 - f) \dot{\mathcal{E}}_{kk}^p + A \dot{\mathcal{E}}^p \quad (3)$$

here,  $\dot{\mathcal{E}}_{kk}^p$  means the mesoscopic plastic strain rate tensor,  $\dot{\mathcal{E}}^p$  is the equivalent plastic strain rate of the matrix materials. The first term in Eqn. 3 arises from the condition of plastic incompressibility of the matrix material. The nucleation of new voids is supposed to obey to a strain-controlled model (cf. Tvergaard [2]):

$$A = \frac{f_N}{s_N \sqrt{2\pi}} \exp \left[ -\frac{1}{2} \left( \frac{\bar{\epsilon}^p - \epsilon_N}{s_N} \right)^2 \right] \quad (4)$$

where  $f_N$  is the volume fraction of void nucleating particles,  $\epsilon_N$  and  $s_N$  are the mean and standard deviation of the strains at which the particles nucleate voids.

#### **Plastic Limit-load Coalescence Model (GTNT)**

Thomason [3] has proposed a critical condition of internal necking in the intervoid ligament at incipient void coalescence. The overall material is then subject to axisymmetric and proportional loading, *i.e.* the mesoscopic principal stresses are  $\Sigma_{33} > \Sigma_{11} = \Sigma_{22}$  and the stress triaxiality ratio  $T = \Sigma_m / \Sigma_{eq}$  is constant. The coalescence condition is given by the loading equilibrium of the intervoid ligament (see Figure 1):

$$\Sigma_{33} \pi L^2 = \pi (L^2 - R^2) \sigma_n \quad (5)$$

where  $\sigma_n$  is the mean stress required to initiate the internal necking in the intervoid matrix materials. Some modifications have been made in Thomason's criterion so as to make it compatible with the GTN model. Firstly, microvoids are assumed to grow spherically. Secondly, plastic-limit load criterion and the GTN model were originally based on a rigid perfect plasticity approach and they were extended to hardening matrix materials by replacing the initial yield stress  $\sigma_0$  with  $\bar{\sigma}$ .

Thomason [3] has proposed an empirical expression for the constraint factor  $\sigma_n / \sigma_0$ , which closely corresponds with the results of the upper-bound theorem for plastic limit-load analysis. Under the second above assumption, the empirical formulation has been transformed into:

$$\frac{\sigma_n}{\bar{\sigma}} = 0.1 \left( \frac{L}{R} - 1 \right)^2 + 1.2 \left( \frac{L}{R} \right)^{1/2} \quad (6)$$

In the case of axisymmetric loading, the critical condition for incipient microvoid coalescence is given by combining Eqn. 5 with Eqn. 6:

$$\left[ 0.1(\alpha^{-1} - 1)^2 + 1.2\alpha^{-1/2} \right] \cdot (1 - \alpha^2) = \frac{\Sigma_{33}}{\bar{\sigma}} \quad (7)$$

$$\alpha = \frac{R}{L} = \left( \frac{3}{2} f \beta \right)^{1/3}; \quad \beta = \frac{H}{L} = \beta_0 \exp \left( \frac{3}{2} E_{eq}^p \right); \quad \beta_0 = \frac{H_0}{L_0}$$

where  $L_0$  and  $H_0$  are the initial radius/width and height of the unit cell. It must be emphasized that  $\Sigma_{33}$ ,  $E_{eq}^p$  and  $f$  in Eqn. 7 are derived from the predictions of the GTN model. In this study, the initial void distribution is homogeneous, *i.e.*  $\beta_0 = 1$  in Eqn. 7.

#### **Localization-based Coalescence Model (GTNP)**

An analytical study of void coalescence by void-sheet mechanism has been carried out by Perrin [4] based on the following assumptions: void distribution becomes inhomogeneous during plastic deformation, then coalescence comes from progressive concentration of cavities in some horizontal porous layers bounded by rigid zones. Perrin has used Rudnicki and Rice's theory [5] of the localization of deformation into the porous layers. The unit cell is subject to mesoscopic axisymmetric loading ( $\Sigma_{33} > \Sigma_{11} = \Sigma_{22}$ ) with a constant triaxiality  $T$  (see Figure 1). The porosity  $f$  and mesoscopic stresses are calculated by applying the GTN model to the overall unit cell. Let  $(\Sigma_{11}^{(p)} = \Sigma_{22}^{(p)}, \Sigma_{33}^{(p)})$  and  $f^{(p)}$  be the mesoscopic principal stresses and porosity in the highly porous layer.

In order to calculate  $f^{(p)}$ , Perrin has assumed that the virtual material, composed by stacking the  $d$ -height

porous layers, is always defined by isotropic void distribution, this entails that  $f^{(p)} = \beta f$  and  $d = 2L$  (see Figure 1b). The vertical equilibrium provides:  $\Sigma_{33}^{(p)} = \Sigma_{33}$ . The behaviour of these  $d$ -height porous layers should adhere to the GTN yield criterion:

$$\left( \frac{\Sigma_{33} - \Sigma_{11}^{(p)}}{\bar{\sigma}} \right)^2 + 2q_1 f^{(p)} \cosh\left( \frac{\Sigma_{11}^{(p)} - \Sigma_{33}/2}{\bar{\sigma}} \right) - 1 - (q_1 f^{(p)})^2 = 0 \quad (8)$$

where  $\Sigma_{11}^{(p)}$  is the only unknown quantity of Eqn. (8), which can be solved by applying a standard numerical method.

Coalescence begins when the strain localization condition is reached inside the porous layers. So, the critical condition at the onset of void coalescence is given by:

$$\frac{3(1-\nu)\bar{\sigma}}{E} q_1^2 (1 - f^{(p)}) f^{(p)} \text{sh}^{(p)} (\text{ch}^{(p)} - q_1 f^{(p)}) = \left( \frac{\Sigma_{33} - \Sigma_{11}^{(p)}}{\bar{\sigma}} - q_1 f^{(p)} \text{sh}^{(p)} \right)^2 \quad (9)$$

where  $\text{sh}^{(p)}$  and  $\text{ch}^{(p)}$  denote the hyperbolic sine and cosine of  $\frac{\Sigma_{11}^{(p)} + \Sigma_{33}/2}{\bar{\sigma}}$ , respectively.

## EXPERIMENTAL PROCEDURE

We have used a ferritic steel 16MND5 (French designation) and an austenitic stainless steel 316L (French designation), which have been studied by Geney [6] at room temperature. Table 1 gives the main chemical composition of these steels. The tensile properties are shown in Table 2. Geney [6] has used an invert resolution method coupled with a FE code in order to determine the stress-strain curves, using experimental data given by round smooth tensile tests, before crack initiation. The tensile tests were carried out by Geney [6] on axisymmetric round notched specimen. The specimen, denoted AE4, has notched radius of 4 mm and an initial minimum diameter of 10 mm (see Figure 2a). This geometry was retained because it allows to generate quasi-homogeneous stress-strain field and a constant stress triaxiality ratio. The tensile tests were performed at the constant speed of 0.5 mm/minute. The reduction of diameter was measured by a diametral extensometer, and the values were recorded with a frequency of 5 Hz.

TABLE 1  
CHEMICAL COMPOSITION IN WEIGHT PERCENT

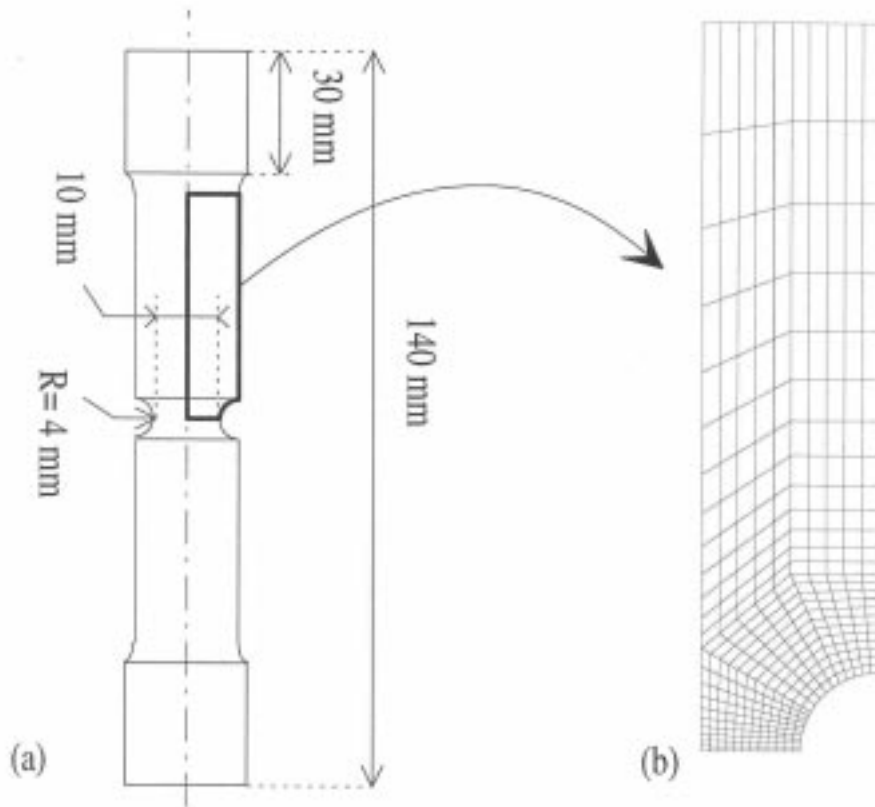
Mat.	C	Mn	Si	S	P	Ni	Cr	Mo	N
16MND5	0,16	1.35	0.21	0.002	0.005	0.74	0.14	0.48	0.004
316L	0.008	0.86	0.63	<0.001	0.011	12.55	17.55	2.40	0.0441

TABLE 2  
MONOTONOUS TENSILE PROPERTIES

Mat.	Temp. (°C)	E (GPa)	$R_{eL}$ (MPa)	$R_{eH}$ (MPa)	$R_{p0.2}$ (MPa)	$R_m$ (MPa)	A (%)	Z (%)
16MND5	20	193	473	475	-	605	25.5	72
316L	20	184	-	-	220	537.5	65	87

## NUMERICAL IMPLEMENTATION AND MODELLING

We have incorporated the GTNT and GTNP models into the FE code CASTEM 2000 [7] by means of two material subroutines. The methodology of implementation could be summarized by the following procedures. Firstly, stresses were updated by using a backward Euler method. Then, the maximum principal stress, the equivalent plastic strain and the porosity were computed and the void coalescence criteria (Eqns. 7 & 9) were tested. Once the coalescence condition is reached in some Gauss points, the critical void volume fraction  $f_c$  is equal to the current porosity and the modification to take account of the void coalescence process (Eqn. 2) becomes effective. So, the critical porosity  $f_c$  is considered as an internal variable.



**Figure 2:** (a) Axisymmetric notched specimen AE4 - (b) FE mesh

Only a half specimen was modelled using axisymmetric 8-nodes isoparametric elements with reduced integration (see Figure 2b). Computations were performed with assuming large strain theory.

## NUMERICAL RESULTS

The GTN model contains a lot of parameters and a generally accepted assent about the determination of these micro-mechanical parameters has to be found. In most cases, some of them should be evaluated from metallurgical observations or set to ‘usual’ values. Then, the other ones are calculated by a purely phenomenological fitting procedure which consists in comparing the numerical prediction of the GTN model with experimental results. As reported by Tvergaard and Needleman [2], the stress carrying capacity drops rapidly once the current porosity reaches the critical void volume fraction  $f_c$ . At this point, the  $f_c$  parameter is calibrated by the fitting procedure. Unfortunately, as reported by Zhang [8], there is a problem of non-uniqueness in this way of parameter fitting.

In pursuing the same idea as Zhang [9], we propose the GTNT and GTNP models in order to avoid this kind of problem by incorporating a ‘physical’ void coalescence process into the GTN model. Within these approaches, the only ‘free’ parameter is the volume fraction of void nucleating particles  $f_N$ . In this study, we have used the

same values of  $q_1$ ,  $q_2$ ,  $f_F$ ,  $\epsilon_N$  and  $s_N$  parameters for both materials. The ‘constitutive’ parameter was set to  $q_1 = 1.25$ , halfway between the original Gurson [1] model (*i.e.*  $q_1 = 1.0$ ) and the modified Gurson model proposed by Tvergaard and Needleman [2] (*i.e.*  $q_1 = 1.5$ ). The parameters for void nucleation were set to  $\epsilon_N = 0.3$  and  $s_N = 0.1$  [2]. The end of void coalescence is described by the final porosity  $f_F = 0.15$ . As regards the initial void volume fraction  $f_0$ , we have assumed nearly the same value as Geney [6], *i.e.*  $f_0 = 5.10^{-5}$  for the 316L material and  $f_0 = 3.10^{-4}$  for the 16MND5 material.

The volume fraction of void nucleating particles  $f_N$  was determined by fitting the numerical results to the experimental data. By using the GTNP model, the fitted  $f_N$ -value was :  $f_N = 3.10^{-3}$  for the 16MND5 steel and  $f_N = 5.10^{-4}$  for the 316L steel. Then, these fitted values of  $f_N$  were used for the GTNT model. The curves of load versus diameter reduction are shown in Figure 3 for both materials. As striction occurs, a loss of stiffness appears and the sustaining load is reduced significantly. Then, the initiation of a macroscopic crack is associated with a sudden drop of the load. It can be seen from Figure 3a & 3b that the GTNP model (dash line) slightly overestimates the sudden drop point of experimental tests (dotted line).

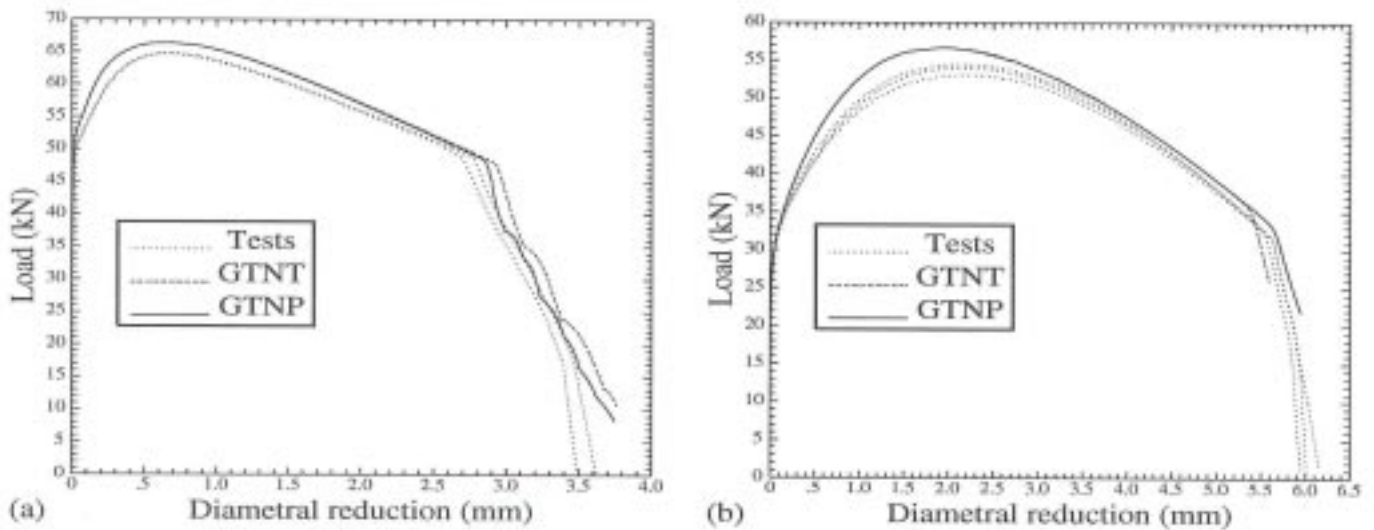


**Figure 3:** Load-diameter reduction curves for steel : (a) 16MND5 and (b) 316L

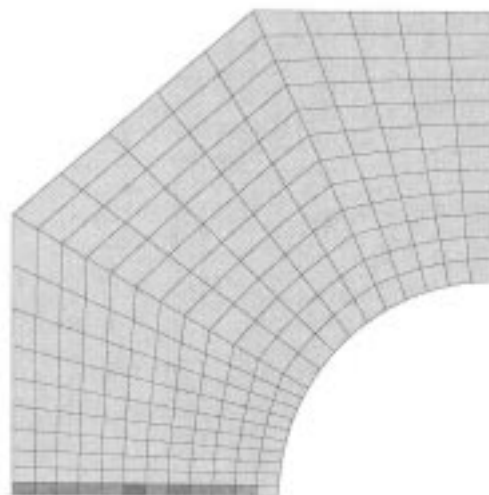


**Figure 4:** Distribution of  $f_c$ -values given by the GTNP model at  $\Delta\phi = 3.75$  mm for the 16MND5 steel

For the four sets of calculations (2 models and 2 materials), damage is localized firstly in the element situated

in the center of the specimen and propagates towards the outer diameter. In the case of  $f_c$ -scalar field computed by the GTNT and GTNP models, we have obtained the same trends. However, coalescence criteria (Eqn. 7 & 9) have provided  $f_c$ -values only located in the minimum section of the specimen. This is illustrated in Figure 4 with contour plots showing the  $f_c$ -values for the diameter reduction  $\Delta\phi = 3.75$  mm. In the four sets of calculations, the first  $f_c$ -values, located next to the middle of the specimen, are nearly constants; and a scattering effect is obtained for the other values in the minimum section of the specimen. The average value of the critical porosity for 16MND5 steel was found to be  $f_c = 2.6\%$  for GTNP model and  $f_c = 1.8\%$  for GTNT model. In the case of 316L steel, we have obtained the following values:  $f_c = 1.1\%$  for GTNP model and  $f_c = 0.8\%$  for GTNT model (see Figure 3b). The  $f_c$ -values coming from the GTNT model are significantly lower than the ones from the GTNP model. In the case of 16MND5 steel, the GTNT model overestimates the starting point of the slope change. For the 16MND5 steel, the average  $f_c$ -values obtained by the GTNT and GTNP models are in quite good agreement with typical values from the literature. For instance, Hao and al. [10] have obtained a critical porosity of  $f_c = 2\%$  for the same type of steel.

## CONCLUSION

Two new models GTNT and GTNP were implemented into the FE code CASTEM 2000. They were tested on two structural steels in order to determine the damage parameters of the GTN model. By using these identification strategies, only one parameter (*i.e.*  $f_N$ ) has to be fitted, while the other ones are selected beforehand. As observed in a previous study based on direct integration of analytical expression of the models [11], the GTNP model seems to provide better results than the GTNT model. It should be noticed that only one type of inclusions was assumed in Thomason and Perrin's coalescence criteria. We have extended phenomenologically these theories to the more general case of materials containing a secondary void family. The application to more complicated fracture specimens with pre-existing crack is currently going on. But, the numerical results are dependent on the mesh-size in fracture mechanics specimens because stress and strain gradients are very steep ahead of a crack tip. So, it becomes necessary to introduce characteristic length parameter(s), related to the average inclusion spacing, into the GTNT and GTNP models.

## ACKNOWLEDGEMENTS

The authors are grateful to Professor S. Degallaix from the "Ecole Centrale de Lille", France, for providing the true stress-strain curves and the experimental data of the axisymmetric round notched tensile specimens.

## REFERENCES

1. Gurson, A.L. (1977) *J. Engng. Mater. Techn.* **99**, 2.
2. Tvergaard, V. and Needleman, A. (1984) *Acta Metall.* **32**, 157.
3. Thomason, P.F. (1984) *Acta Metall.* **33**, 1079.
4. Perrin, G. (1992). PhD Thesis, Ecole Polytechnique, Paris.
5. Rudnicki, J.W. and Rice, J.R. (1975) *J. Mech. Phys. Solids* **23**, 371.
6. Geney, Ch. (1998). PhD Thesis, Ecole Centrale de Lille, France.
7. Millard, A. (1993). CASTEM 2000: Guide d'utilisation, CEA, Internal Report, France.
8. Zhang, Z.L. and Hauge, M. (1996). In: *ECF11 European Conference on Fracture*, pp. 941-946, 3 – 6 September, Poitiers, France.
9. Zhang, Z.L. and Niemi, E. (1995) *Int. J. Fracture* **70**, 321.
10. Hao, S., Brocks, W., Heerens and Hellmann, D. (1996). In: *ECF11 European Conference on Fracture*, pp. 929-934, 3 – 6 September, Poitiers, France.
11. Chambert, J., Bressolette, Ph. and Vergne, A. (1999). In: *ECCM'99 European Conference on Computational Mechanics*, August 31 – September 3, München, Germany.